Pergamon

Int. J. Heat Mass Transfer. Vol. 37, No. 16, pp. 2415–2424, 1994

0017-9310/94 $7.00 + 0.00

0017-9310(94)E0087-B

Numerical prediction of forced convection film boiling heat transfer from a sphere

K. H. BANG

Department of Mechanical Engineering, Pohang Institute of Science and Technology, Pohang, Korea

(*Received* 26 *August* 1993 *and in final form* 10 *March* 1994)

Abstract—Forced convection film boiling over a sphere is modeled by applying the laminar boundary-layer approximation for both the vapor and liquid flows. In the vapor momentum equation, a buoyancy term is included, which has often been neglected in past analyses. The solution is obtained numerically to the point of flow separation. From the analysis of forced convection film boiling over a sphere submerged in water, it is shown that the vapor film thickness is in the submillimeter range, and as the subcooling of liquid increases, the film thickness becomes thinner, down to the order of ten microns. It is also observed that the buoyance force may not be neglected in the liquid velocity range considered in this study (up to 7 m s^{-1}). The heat transfer results of the present model agree qualitatively with available experimental data, although quantitatively the model generally underestimates the data. Using the results of the present analysis, an improved correlation for the convective heat transfer to the bulk liquid in subcooled film boiling of a sphere in water is proposed for use in predicting the vapor generation rate.

1. INTRODUCTION

FILM boiling heat transfer from a hot spherical body submerged in a liquid is often encountered in many engineering problems. In particular, the analysis of quenching and the violent interaction of a molten core in contact with water during a postulated nuclear reactor accident requires a heat transfer rate from a moving droplet in water [1, 2]. Film boiling from a moving sphere or a sphere submerged in flowing liquid differs from pool film boiling in the way that the vapor flow field is affected by the momentum exchange with the liquid flow at the vapor–liquid interface in addition to the buoyance force.

An analytical treatment of flow film boiling was first made by Bromley [3] for a vertical surface by balancing the gravitational buoyance force and fluid shear stress. He assumed a linear temperature profile in the vapor and drove an analytical form of heat transfer coefficient. Cess and Sparrow [4] treated forced convection film boiling on a horizonal flat plate as a self-similar problem by assuming laminar boundary-layer flow.

Forced convection film boiling over bluff bodies such as cylinders and spheres makes its analytical treatment more difficult because of flow separation and wake formation. Kobayasi [5] solved forced convection film boiling heat transfer from a sphere by assuming a linear temperature profile in the vapor film and a nonlinear vapor velocity profile resulting from liquid pressure variation. The effect of a nonlinear vapor velocity profile was later examined by Witte and Orozco [6]. They showed that accounting for the nonlinearity of the vapor velocity yields a better prediction of the experimental data. However, it is noted that they assumed that the buoyance force is negligible and the liquid velocity at the liquid–vapor interface is unaffected by vapor drag.

Shigechi *et al.* [7] proposed an integral method of boundary-layer equations including the buoyance term for flow film boiling from cylinders and spheres, and the effect of radiation was investigated. They neglected the inertia term in the vapor momentum equation and a linear vapor temperature was assumed. Their parametric study of radiation effect showed that the radiation contribution becomes more significant as the liquid subcooling increases. However, because the liquid is semi-transparent to thermal radiation, a more detailed modeling of the liquid energy equation, including the radiation absorption by bulk liquid, is needed for better prediction of the radiation effect. In the later paper by Shigechi *et al.* [8], an analytical solution of film boiling heat transfer from a cylinder for the integral boundary-layer equations was proposed. They investigated the effect of vapor velocity and temperature profiles parametrically using four different cases of assumed profiles. They reported that their results showed good agreement with the experimental data with ethanol, but underestimated the data with R-113.

The effect of buoyance force in forced convection film boiling from a sphere can be neglected if the liquid velocity is high. However, for a low or moderate range

NOMENCLATURE

a	sphere radius
c_p	specific heat
D	sphere diameter
g_0	gravitational acceleration
Gr	Grashof number, $D^3 g_0 \rho \Delta\rho/\mu^2$
h	heat transfer coefficient
h_{fg}	latent heat of vaporization
Ja	Jacob number, $c_p \Delta T/h_{fg}$
k	thermal conductivity
Nu	Nusselt number, hD/k_v
Nu_r	Nusselt number of radiation, $h_r D/k_v$
Pr	Prandtl number, $c_p \mu/k$
Re	Reynolds number, $U_\infty D/v$
T	temperature
ΔT_w	$T_w - T_{sat}$
ΔT_b	$T_{sat} - T_0$.

Greek symbols

α_T	thermal diffusitivity, $k/\rho c_p$
α	radiation absorptivity
δ	vapor film thickness
ε	radiation emissivity
ρ	density
$\Delta\rho$	$\rho_l - \rho_v$
μ	dynamic viscosity
v	kinematic viscosity.

Subscripts

0	free stream property
∞	bulk liquid property
l	liquid
NC	natural convection
r	radiation heat transfer
sat	saturation
v	vapor
w	wall.

of liquid velocity, in particular if the sphere or liquid is moving in the direction of gravity, the buoyance force can be comparable to the pressure gradient and viscous shear force. Thus, the velocity of the liquid–vapor interface can be larger or smaller than the free stream liquid velocity depending on the magnitude of the buoyance term. The temperature profile in both the vapor and liquid regions also becomes important if the liquid is subcooled. In order to include the above effects properly, a complete set of conservation equations of mass, momentum, and energy in both the vapor and liquid regions must be solved.

In this paper, forced convection film boiling over a sphere is modeled by applying the laminar boundary-layer approximation for both the vapor and liquid flows. The solution is obtained numerically to the point of flow separation, and the effect of the buoyance term and comparison with the available experimental data are discussed. The mathematical symbols are defined in the nomenclature list.

2. MODEL FORMULATION

2.1. *Governing equations*

The basic flow model is shown in Fig. 1. The models are based on the following assumptions:

(1) pure, incompressible liquid and vapor
(2) smooth liquid–vapor interface with laminar vapor and liquid flows
(3) uniform surface temperature
(4) thin vapor film compared with the size of sphere
(5) constant thermophysical properties
(6) thermal radiation absorption is included only at the liquid–vapor interface.

The velocity and temperature distributions in both vapor and liquid phases are governed by the principles of mass, momentum, and energy conservation. For the case of steady, axisymmetric flow, the boundary-layer form of the conservation laws is

$$\frac{\partial ru}{\partial x} + \frac{\partial rv}{\partial y} = 0 \tag{1}$$

$$u\frac{\partial u}{\partial x} + v\frac{\partial u}{\partial y} = U_0\frac{dU_0}{dx} + v\frac{\partial^2 u}{\partial y^2} + \frac{\Delta\rho}{\rho} g_0 \sin\left(\frac{x}{a}\right) \tag{2}$$

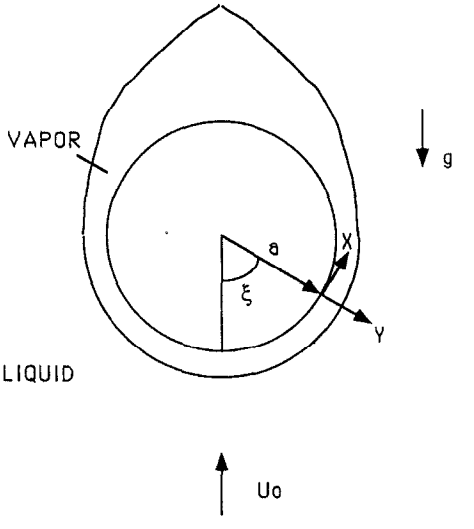

FIG. 1. Model of forced convection film boiling from a sphere.

$$u\frac{\partial T}{\partial x}+v\frac{\partial T}{\partial y}=\alpha_T\frac{\partial^2 T}{\partial y^2}. \tag{3}$$

Equations (1)–(3) apply to both vapor and liquid phases, except for the buoyance term in the liquid momentum equation, and thus the subscript v (vapor) or l (liquid) is omitted in the properties.

To complete the description of the problem, it is necessary to give the conditions of continuity at the liquid–vapor interface and the boundary conditions. At the interface between liquid and vapor, it is required that the continuity be preserved for the following flow-connected quantities: (a) tangential velocity; (b) tangential shear, and (c) mass-flow crossing interface. The continuity requirements on quantities (a), (b) and (c) are equivalent to imposing the following equations within the limit of boundary-layer assumptions as already practised by Cess and Sparrow [4]:

$$u_{liq}=u_{vap} \tag{4}$$

$$\mu_l\left(\frac{\partial u}{\partial y}\right)_{liq}=\mu_v\left(\frac{\partial u}{\partial y}\right)_{vap} \tag{5}$$

$$\rho_l\left(u\frac{d\delta}{dx}-v\right)_{liq}=\rho_v\left(u\frac{d\delta}{dx}-v\right)_{vap}. \tag{6}$$

In addition, the interface temperature is the saturation temperature of the fluid

$$T_l=T_v=T_{sat}. \tag{7}$$

The boundary conditions at the sphere surface and in the undisturbed flow are

$$\begin{aligned} &y=0: \quad u=v=0 \quad T=T_w\\ &y\to\infty: \quad u\to U_0 \quad T=T_0. \end{aligned} \tag{8}$$

These matching and boundary conditions, together with the conservation laws, provide a complete statement of the problem. Now efforts can be directed towards transforming the governing equations into a more tractable form and then finding solutions.

2.2. *Similarity transformation*

To bring the problem into a more tractable form, the continuity and momentum equations can be combined into a single third-order equation in terms of a stream function, and the resulting equations can undergo the change of variables by means of the Falkner–Skan transformation [9].

For the vapor phase, the new variables are defined by

$$\eta=y\sqrt{\left(\frac{U_0}{\nu_v x}\right)} \qquad \xi=\frac{x}{a}$$

$$f(\eta,\xi)=\frac{\psi}{\sqrt{(\nu_v U_0 x)}} \quad \theta(\eta,\xi)=\frac{T-T_{sat}}{T_w-T_{sat}}. \tag{9}$$

From this, it follows that

$$u=\frac{1}{r}\frac{\partial r\psi}{\partial y}=U_0 f' \tag{10}$$

$$v=-\frac{1}{r}\frac{\partial r\psi}{\partial x}=\frac{1}{2}\sqrt{\left(\frac{\nu_v U_0}{x}\right)}\left(\eta f'(1-M)-f(1+M+2R)-2x\frac{\partial f}{\partial x}\right) \tag{11}$$

where the primes ($'$) denotes differentiation with respect to the independent variable η, and

$$M=\frac{\xi}{U_0}\frac{dU_0}{d\xi} \quad R=\frac{\xi}{r}\frac{dr}{d\xi}. \tag{12}$$

For a sphere, the transverse radius r is expressed explicitly as

$$r(\xi)=a\sin\xi. \tag{13}$$

Correspondingly, for the liquid phase, the new variables are

$$\zeta=y\sqrt{\left(\frac{U_0}{\nu_l x}\right)} \qquad \xi=\frac{x}{a}$$

$$F(\zeta,\xi)=\frac{\Psi}{\sqrt{(\nu_l U_0 x)}} \quad \Theta(\zeta,\xi)=\frac{T-T_0}{T_{sat}-T_0} \tag{14}$$

with the velocities given by

$$u=\frac{1}{r}\frac{\partial r\Psi}{\partial y}=U_0 F' \tag{15}$$

$$v=-\frac{1}{r}\frac{\partial r\Psi}{\partial x}=\frac{1}{2}\sqrt{\left(\frac{\nu_l U_0}{x}\right)}\left(\zeta F'(1-M)-F(1+M+2R)-2x\frac{\partial F}{\partial x}\right). \tag{16}$$

In this instance the primes represent differentiation with respect to ζ.

When the transformations defined by equations (9)–(16) are introduced into the conservation equations (2) and (3) for the vapor and liquid phases respectively, the results are:

$$f'''+\left(\frac{M+1}{2}+R\right)ff''+M(1-f'^2)=\xi\left(f'\frac{\partial f'}{\partial\xi}-f''\frac{\partial f}{\partial\xi}\right)-\frac{Gr_v}{2Re_v^2}\frac{\xi\sin\xi}{(U_0/U_\infty)^2} \tag{17}$$

$$\theta''+Pr_v\left[\xi\frac{\partial f}{\partial\xi}+f\left(\frac{M+1}{2}+R\right)\right]\theta'=Pr_v\xi f'\frac{\partial\theta}{\partial\xi} \tag{18}$$

$$F'''+\left(\frac{M+1}{2}+R\right)FF''+M(1-F'^2)=\xi\left(F'\frac{\partial F'}{\partial\xi}-F''\frac{\partial F}{\partial\xi}\right) \tag{19}$$

$$\Theta'' + Pr_l\left[\xi\frac{\partial F}{\partial \xi} + F\left(\frac{M+1}{2} + R\right)\right]\Theta' = Pr_l \xi F' \frac{\partial \Theta}{\partial \xi}. \quad (20)$$

The matching and boundary conditions may also be rewritten in terms of the new variables. First, it may be noted that, at the interface, $y = \delta$ (see Fig. 1), and correspondingly the value of η at the interface is denoted as η_δ. The interfacial value of ζ might also be denoted as ζ_δ. However, since the actual value of ζ does not enter the governing equations, neither in the differential equations (19) and (20) nor in the boundary conditions, it can be taken, without any loss of generality, that $\zeta = 0$ at the liquid–vapor interface. From equations (4)–(6), the matching conditions at the interface in terms of the new variables are

$$F(0) = \sqrt{\left(\frac{\rho_v \mu_v}{\rho_l \mu_l}\right)} f(\eta_\delta)$$

$$F'(0) = f'(\eta_\delta)$$

$$F''(0) = \sqrt{\left(\frac{\rho_v \mu_v}{\rho_l \mu_l}\right)} f''(\eta_\delta)$$

$$\Theta(0) = 1$$

$$\theta(\eta_\delta) = 0. \quad (21)$$

The boundary conditions at the sphere surface and in the free stream are

$$\eta = 0: \quad f(0) = f'(0) = 0 \quad \theta(0) = 1$$

$$\zeta \to \infty: \quad F' \to 1 \qquad \Theta \to 0. \quad (22)$$

From an energy balance at the interface.

$$\left(-k\frac{\partial T}{\partial y}\right)_{vap} - \left(-k\frac{\partial T}{\partial y}\right)_{liq} + q_r'' = \dot{m} h_{fg} \quad (23)$$

where q_r'' is the radiation heat flux at the interface, $\dot{m}$ is the mass flow across the interface and h_{fg} is the latent heat of vaporization. q_r'' is written as

$$q_r'' = h_r(T_w - T_{sat}) \quad (24)$$

where the heat transfer coefficient by radiation (h_r) is given by

$$h_r = \frac{\sigma}{1/\varepsilon_w + 1/\alpha_l - 1}\frac{(T_w^4 - T_{sat}^4)}{(T_w - T_{sat})} \quad (25)$$

and σ is the Stefan–Boltzmann constant.

Taking $\dot{m}$ from the right side of equation (6) and using the new variables, equation (23) becomes

$$\frac{Ja_v}{Pr_v}[-\theta'(\eta_\delta)] - \frac{Ja_l}{Pr_l}[-\Theta'(0)]\sqrt{\left(\frac{\rho_l \mu_l}{\rho_v \mu_v}\right)}$$

$$+ \frac{Nu_r}{\sqrt{(Re_v)}}\left(\frac{Ja_v}{Pr_v}\right)\sqrt{\left(\frac{\xi}{2(u_0/u_\infty)}\right)}$$

$$= f'(\eta_\delta)\xi\frac{d\eta_\delta}{d\xi} + \tfrac{1}{2}f(\eta_\delta)(1+M+2R) + \xi\left.\frac{\partial f}{\partial \xi}\right|_{\eta_\delta}. \quad (26)$$

The differential equations (17)–(20) together with the interface and boundary conditions (21) and (22) provide a complete set for determining the velocity and temperature profiles of the vapor and liquid flows. The interfacial energy balance of equation (26) is used to determine the vapor film thickness. From the above analysis, it is shown that the forced convection film boiling heat transfer coefficient depends on such parameters as:

$$Nu \equiv \frac{hD}{k_v} = f\left\{Re_v, Gr_v, Pr_v, Pr_l, Ja_v, Ja_l, Nu_r, \frac{\rho_v \mu_v}{\rho_l \mu_l}\right\}. \quad (27)$$

2.3. *Solution procedure*

A computer program was written to solve the differential equations (17)–(20) numerically. The third-order differential equations of the momentum equations (17) and (19) are reduced to a set of second-order and first-order equations such that

$$f' = u \quad (28)$$

$$u'' + \gamma f u' + \delta(1-u^2) = \beta\left(u\frac{\partial u}{\partial \xi} - u'\frac{\partial f}{\partial \xi}\right) - \epsilon \quad (29)$$

where the coefficients γ, δ, β, and ϵ represent the corresponding constants in equations (17) and (19), respectively. The nonlinear terms $u'f$ and u^2 are linearized such that

$$u'f = u'f_* + u_*'f - u_*'f_* \quad (30)$$

$$u^2 = 2uu_* - u_*u_*. \quad (31)$$

u_* and f_* are initially guessed values and u and f are from the previous iteration during the iterative solution procedure.

The differential equations are rewritten in the finite-difference form using the central-difference scheme in the η direction and the backward-difference scheme in the ξ direction. The momentum and energy equations for both vapor and liquid are solved consecutively. With a guessed vapor film thickness, the implicit solutions of velocity and temperature in the η direction are first obtained by two-step forward and backward sweeps from the tri-diagonal form of the difference equations, and this procedure is repeated with the corrected vapor film thickness until the interfacial energy balance (equation (26)) is satisfied. This solution procedure is forwarded in the ξ direction starting from the stagnation point until the flow-separation occurs.

The local heat flux at the sphere surface is

$$q'' = \left(-k\frac{\partial T}{\partial y}\right)_{vap,w} + q_r''. \quad (32)$$

Using the definition of $h = q''/(T_w - T_{sat})$ and the new variables, the local Nu number is

$$Nu = \sqrt{(2Re_v)[-\theta'(0)]}\sqrt{\left(\frac{u_0/u_\infty}{\xi}\right)} + Nu_r. \quad (33)$$

The free stream velocity variation was taken from the potential flow result, which is

$$\frac{u_0}{u_\infty} = \tfrac{3}{2}\sin\xi. \quad (34)$$

3. RESULTS AND DISCUSSION

The forced convection film boiling from a sphere submerged in water was analyzed using the present model. The current model is not limited to solid spheres, but attention must be given when applying it to a liquid drop because the internal flow inside the drop, if it exists, is not accounted for here. The thermophysical properties used in the calculation are evaluated at the film temperature.

3.1. *Vapor film thickness*

Figure 2 shows the vapor film thickness variation around the 20 mm diameter sphere for different liquid subcooling. The inclusion of radiation heat transfer increases the vapor film thickness due to larger vapor generation. It is noted that black-body radiation parameters are used in the present analysis to evaluate the maximum contribution by radiation rather than leaving the radiation quantity parametric due to the semi-transparent nature of the liquid to thermal radiation. For saturated water, the vapor film thickness lies in the range of 0.2 mm and thinning of the film thickness is observed as the liquid temperature decreases. At high liquid subcooling, the film thickness approaches the order of ten microns. This indicates that the surface roughness of the sphere becomes important in the film boiling heat transfer in highly subcooled liquid, and thus care must be taken in experimental heat transfer measurements to provide consistent surface conditions.

In the subcooled liquid flow, the flow separation occurs in the liquid side first and the point of flow separation moves towards the stagnation point as the liquid subcooling decreases. For saturated water, the flow separation occurs much later due to increasing vapor velocity driven by the sizable buoyance force, i.e. the interface velocity is larger than the free stream liquid velocity. The typical velocity profile in this case is shown in Fig. 3 for the vapor and liquid layer together at four different angles along the sphere. Noting that most previous investigators used an assumed vapor velocity profile, or a parametric study by Shigechi *et al.* [8], the vapor velocity profiles in this figure do not seem to be similar along the angle when the buoyance term is not negligible. For subcooled liquids, the interface velocity generally appears smaller than the free stream liquid velocity. The temperature profile in the vapor film is very close to linear, as shown in Fig. 4.

3.2. *Heat transfer*

Figure 5 shows the local heat transfer coefficient for different liquid subcooling. The higher heat transfer at larger liquid subcooling is due to the thinner vapor film and the convective heat transfer to the bulk liquid. It is noted that the step changes in the result of higher liquid subcooling in this figure are due to the discretization of vapor film in the numerical method. In

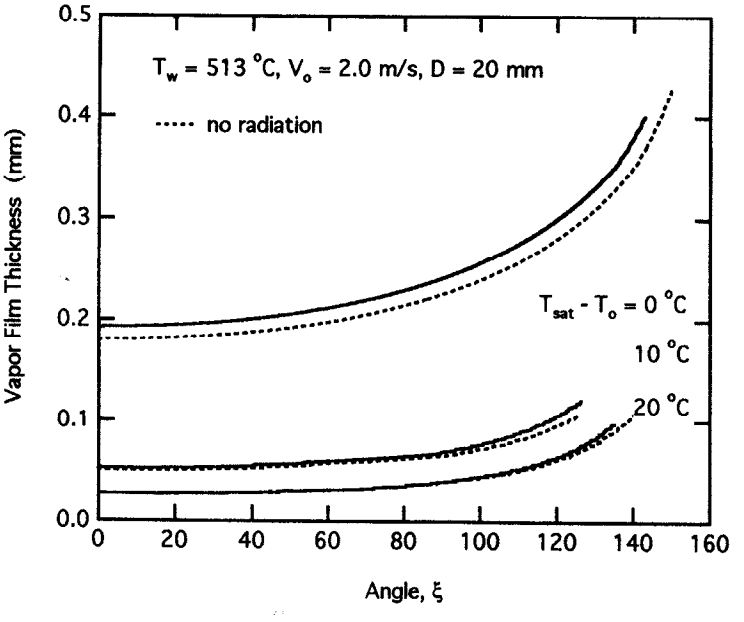

FIG. 2. Vapor film thickness profile around a sphere in water.

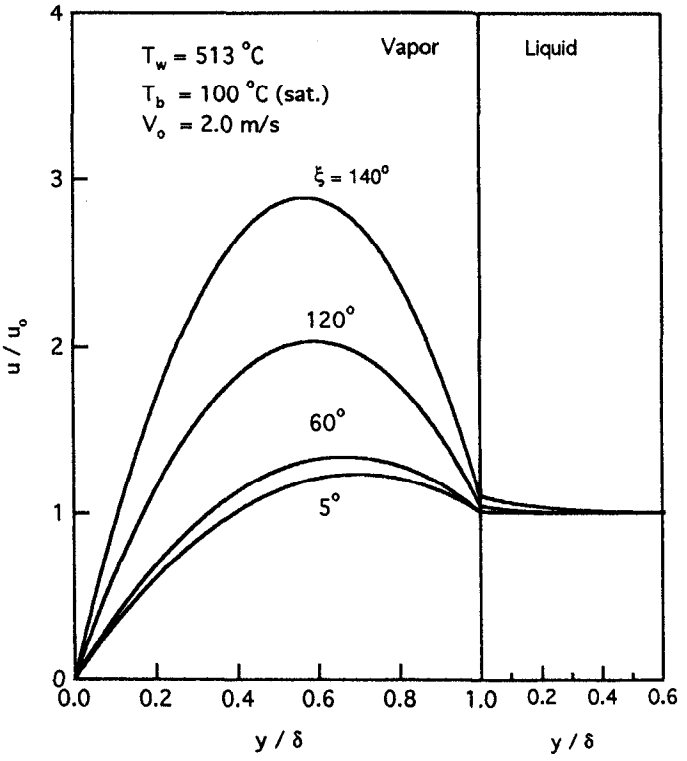

FIG. 3. Velocity profiles of vapor and liquid around sphere in water.

this case, the cell size ($\Delta\eta$) is 0.0025. The effect of cell size in the η direction was examined by picking $\Delta\eta = 0.005$, 0.001, and 0.0005, and the difference in overall heat transfer appears negligible.

The effect of radiation seems apparent in saturated water, but it is a negligible amount if the liquid is subcooled. For the saturated water in this figure, the heat transfer coefficients at the stagnation point are

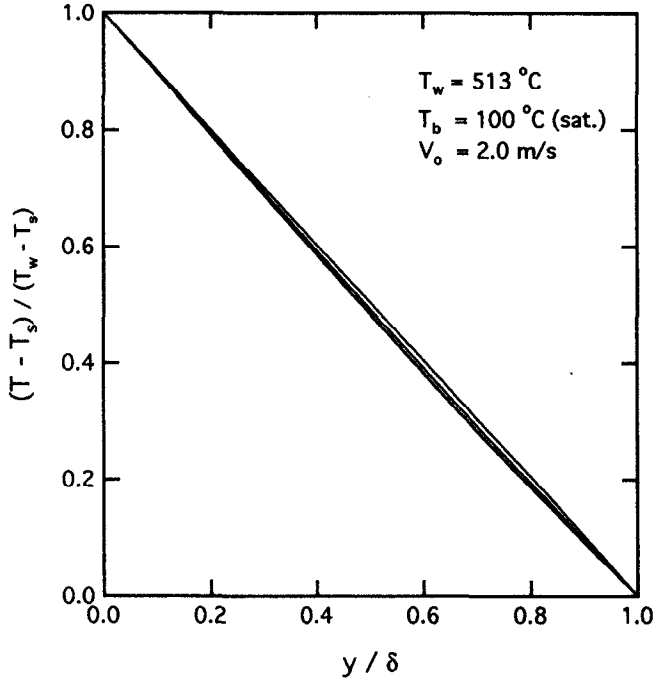

FIG. 4. Vapor temperature profiles at ξ = 5, 60, 120, 140°.

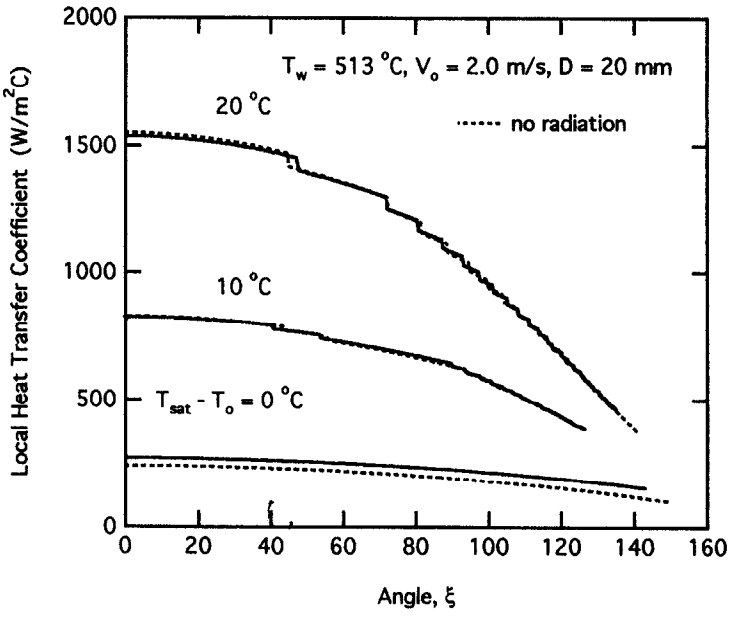

FIG. 5. Local heat transfer coefficient around sphere in water.

increased by 35 W m^{-2} K^{-1} due to radiation. The radiative heat transfer alone is 49 W m^{-2} K^{-1} in this case, thus the net radiation effect $((h-h_{norad})/h_{rad})$ is 0.72. For 20°C subcooled water, this number is 0.2. From the analysis of the radiation effect by Shigechi *et al.* [7], this number for a sphere velocity of 2 m s^{-1} is around 0.9 for saturated water and 0.4 for 20°C subcooled liquid. Therefore, the present model shows smaller radiation effect than Shigechi's analysis.

The effect of buoyance force in the vapor flow is shown in Fig. 6. It is seen that the underestimation of heat transfer by neglecting the buoyance term becomes larger as the sphere velocity (or liquid velocity) decreases. At a sphere velocity of 2 m s^{-1}, which is close to the terminal velocity of a sphere of 20 mm in diameter falling in water, the underestimation amounts to about 30%. It is noted that the buoyance term was often neglected in previous work [5, 6] even in this range of sphere velocity. The result of pool film boiling obtained elsewhere [10] is compared in the figure, indicating that the present result approaches it as the sphere velocity decreases.

The experimental data of forced convection film boiling from a sphere are scarce. Among the limited data, the data of Orozco and Witte [11] is for Freon-11, the boiling characteristics of which are significantly different from water. The data of Dhir and Purohit [12] and Aziz [13] are for water. These data were obtained by the quenching of a hot solid sphere moving in water. However, these data cover the narrow range of sphere velocity (0–1.8 m s^{-1}). The comparison of the current analysis with these two experimental data is shown in Fig. 7. In this comparison, the solid line was obtained by using the superheated vapor properties at one atmospheric pressure and film temperature, which is the average of saturation temperature and the wall temperature. The dotted line is obtained by using vapor thermal conductivity at the saturation condition at the film temperature. It is first observed that there is a large difference even among the present analyses depending on the properties used.

In general, the comparison shows qualitative agreement, but it is also noted that a large difference exists even between the two experimental data. In order to properly explain the difference, there are a couple of points to mention. The experimental data shown here were both obtained during the quenching of a preheated sphere and the heat transfer coefficients were calculated by solving the inverse conduction problem, knowing the measured temperature at the center of the sphere. Therefore, a large scatter of the data obtained in this way may result, depending on the time at which the data were taken and the thermophysical properties used in the data reduction.

Second, the liquid–vapor interface in film boiling tends to be wavy compared with the smooth interface assumed in the present model. The wavy interface can increase the heat transfer rate significantly due to a larger heat transfer area and more complex flow field. This is one of the resons why the present analysis underestimates the experimental data. Another source of the underestimation is the fact that the present analysis does not cover the area beyond the flow separation point while the average heat transfer coefficient shown here is based on the whole surface area of the sphere. Although it is generally believed that the heat transfer in the wake area—the vapor dome—is small compared with the vapor film region, it is the area, together with the inclusion of the effect of the wavy interface, for future improvement of the

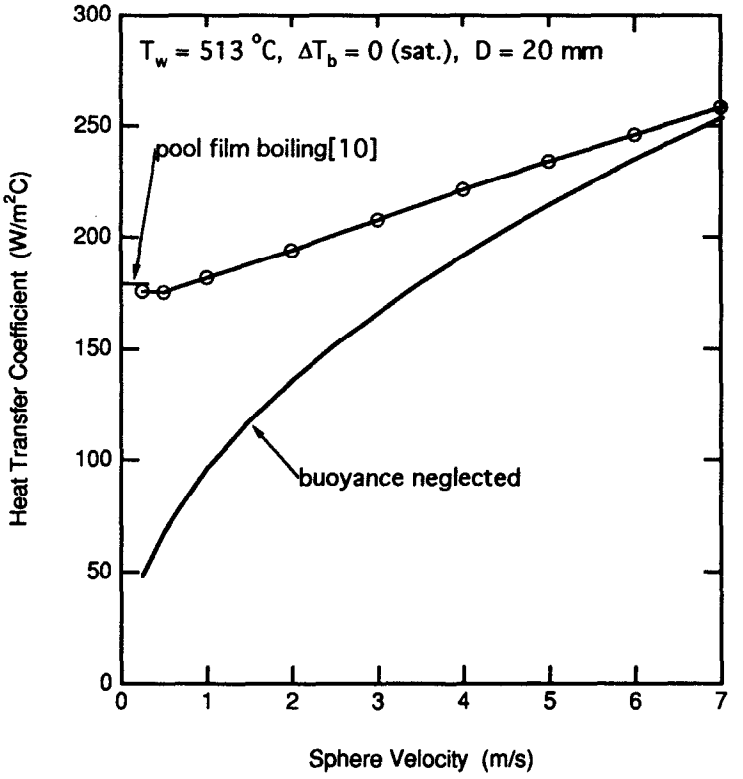

FIG. 6. The effect of buoyance force on heat transfer.

model to predict the experimental data more accurately.

3.3. *Convective heat transfer to bulk liquid*

In the analysis of film boiling heat transfer, in particular in a subcooled liquid, not only the total heat transfer from the sphere, but also the convective heat transfer to the bulk liquid is of concern when the quantity of the vapor generation rate is required, as is the case of multiphase flow field computation in which boiling heat transfer is involved. In such a case, it has been a common practice to calculate the vapor generation rate using the net heat transfer rate at the liquid–vapor interface, i.e. subtraction by the convective heat loss to the bulk liquid from the total heat transfer from the sphere. However, the amount of convective heat transfer to the liquid in film boiling is very difficult to measure experimentally, so no data have been reported in the literature. Therefore, in solving such a problem, the data of single-phase convection heat transfer are often used, for example, as in ref. [1].

One of the commonly used correlations of single-phase convective heat transfer from a sphere is Ranz and Marshall's [14] as shown in Fig. 8. The major drawback of this correlation in applying it to the film boiling problems discussed above is that it is based on the no-slip condition at the wall, which is different from the condition at the liquid–vapor interface. In the present analysis, the convective heat transfer to the bulk liquid is obtained and the result is well correlated in terms of liquid Reynolds number as shown in Fig. 8:

$$\frac{Nu_l - Nu_{NC}}{Pr_l^{1/3}} = CRe_l^{1/2} \tag{35}$$

where C is 1.1 ± 0.05 for water. Nu_{NC} is 2.0 from the exact solution of natural convection heat transfer over a sphere [14]. As seen in the figure, the use of Ranz and Marshall's correlation underpredicts the convective heat transfer to the liquid in subcooled film boiling by about 50%, thus causing excessive vapor generation as pointed out in the past analysis [1]. It is noted that equation (35) is based on the present model and it is suggested that it should only be applied to water. It should be validated with experimental data if available in the future.

4. CONCLUSION

Forced convection film boiling over a sphere is modeled by applying the laminar boundary-layer approximation for both the vapor and liquid flows. The momentum equations are transformed into third-order differential equations and the solution is obtained numerically to the point of flow separation. In the vapor momentum equation, a buoyance term is included, which has been often neglected in past analyses.

The analysis of forced convection film boiling over a sphere submerged in water shows that the vapor film

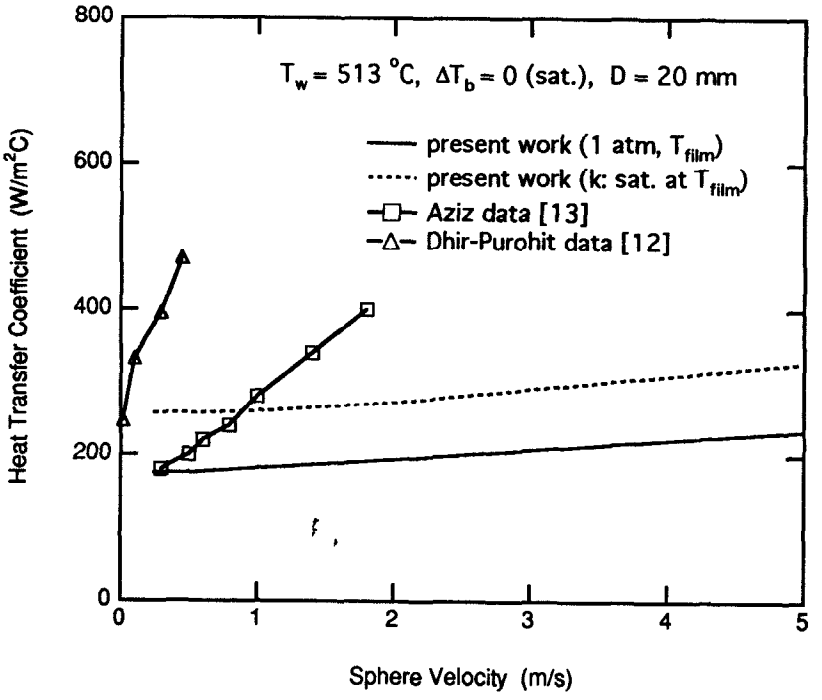

FIG. 7. Heat transfer comparison with experimental data.

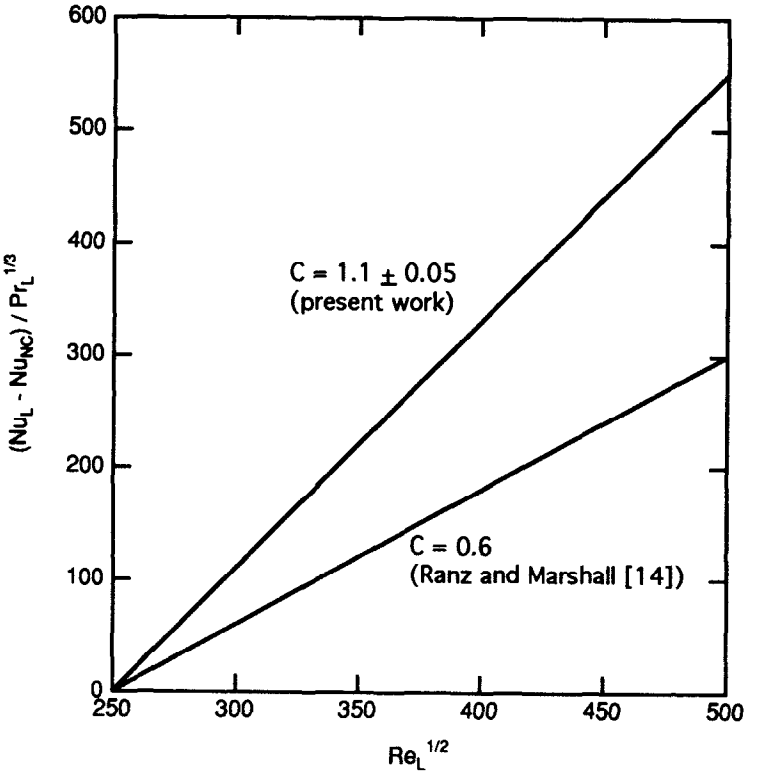

FIG. 8. Convective heat transfer to bulk liquid in subcooled flow film boiling of sphere in water.

thickness is in the submillimeter range, and as the subcooling of liquid increases, the film thickness becomes thinner, down to the order of ten microns at which point the surface roughness becomes important. It is also observed that the buoyance force may not be neglected in the liquid velocity range considered in this study (up to 7 m s^{-1}).

The heat transfer results of the present model agree qualitatively with available experimental data, although the model generally underestimates the data.

The reasons for the underestimation seem to be that the present model does not account for a wavy liquid–vapor interface and it is unable to solve the area beyond the flow separation point. Using the results of the present analysis, an improved correlation for the convective heat transfer to the bulk liquid in subcooled film boiling of a sphere in water is proposed for use in predicting the vapor-generation rate. While improved experimetnal data, such as could be obtained from steady-state experiments, are required for the model validation, the present model can be improved by including the effect of wavy interface and extending the solution to the wake region, for which the modeling of more complex phenomena seems in order.

Acknowledgement—The author wishes to thank the Advanced Fluids Engineering Research Center at the Pohang Institute of Science and Technology for the computer support for this study.

REFERENCES

1. C. C. Chu and M. L. Corradini, One-dimensional transient fluid model for fuel/coolant interaction analysis, *Nucl. Sci. Engng* **101,** 48–71 (1989).
2. D. Magallon and H. Hohmann, High pressure corium melt quenching tests in FARO, *CSNI–FCI Specialists Mtg.*, Santa Barbara (1993).
3. L. A. Bromley, Heat transfer in stable film boiling, *Chem. Engng Prog.* Ser. 46, 221–227 (1950).
4. R. D. Cess and E. M. Sparrow, Film boiling in a forced-convection boundary-layer flow, *ASME Heat Transfer*, August, 370–376 (1961).
5. K. Kobayasi, Film boiling heat transfer around a sphere in forced convection, *J. Nucl. Sci. Technol.* **2,** 62–67 (1965).
6. L. C. Witte and J. A. Orozco, The effect of vapor velocity profile shape on flow film boiling from submerged bodies, *J. Heat Transfer* **106,** 191–197 (1984).
7. T. Shigechi, T. Ito and K. Nishikawa, The effect of radiation on film boiling heat transfer: horizontal cylinder and sphere perpendicular to upward vertical flow, *Bull. Jap. Soc. Mech. Engrs* **29,** 489–494 (1986).
8. T. Shigechi, N. Kawae, K. Kanemaru and T. Yamada, Forced convection film boiling heat transfer from a horizontal cylinder to saturated liquid cross-flowing upward. In *Advances in Phase Change Heat Transfer*, pp. 203–208. International Academic Publishers (1988).
9. H. Schlichting, *Boundary-Layer Theory* (7th Edn). McGraw-Hill, New York (1979).
10. V. P. Carey, *Liquid–Vapor Phase-Change Phenomena.* Hemisphere, Washington, DC (1992).
11. J. A. Orozco and L. C. Witte, Flow film boiling from a sphere to subcooled Freon-11, *ASME J. Heat Transfer* **109,** 934–938 (1986).
12. V. K. Dhir and G. P. Purohit, Subcooled film-boiling heat transfer from spheres, *Nucl. Engng Design* **47,** 49–66 (1978).
13. S. Aziz, Forced convection film boiling on spheres, Ph.D. Thesis, University of Oxford (1989).
14. R. B. Bird, W. E. Stewart and E. N. Lightfoot, *Transport Phenomena.* Wiley, New York (1960).